Journal of Power Sources 186 (2009) 320–327

Contents lists available at ScienceDirect

Journal of Power Sources

journal homepage: www.elsevier.com/locate/jpowsour

A study on novel pulse preparation and electrocatalytic activities of Pt/C-Nafion electrodes for proton exchange membrane fuel cell

Jingjing Li, Feng Ye, Ling Chen, Tongtao Wang, Jianling Li, Xindong Wang*

Department of Physical Chemistry, University of Science and Technology Beijing, Beijing 100083, China

ARTICLE INFO

Article history:
Received 15 May 2008
Received in revised form 14 July 2008
Accepted 16 July 2008
Available online 23 July 2008

Keywords:
PEMFC
Pt catalyst
Electrodeposit
Oxygen reduction reaction (ORR)
Hydrogen underpotential deposition (H-UPD)

ABSTRACT

To aim at reducing the platinum loading and increasing the utilization of platinum in PEMFC electrode, a new pulse electrodeposition technique for preparing proton exchange membrane fuel cell (PEMFC) electrodes has been developed in this paper. This method combines coating Pt seeds on the C-Nafion substrate and introducing polyethylene glycol (PEG) into the deposition solution. SEM images of the samples show that Pt seeds and PEG take an important role in the morphology of the Pt deposit. The surface area and average particle size of Pt were determined by charge integration under the hydrogen desorption peaks of cyclic voltammetry. The electrocatalytic activities of these electrodes towards oxygen reduction reaction (ORR) were investigated by using rotating disc electrode (RDE). The Pt catalyst which was prepared by Pt seeds and PEG, its active surface area and electrocatalytic activity towards ORR were improved remarkably. And the optimized electrode displayed higher catalytic activity than a conventional electrode made from commercial Pt/C catalyst. The possible reasons for the effects of Pt seeds and PEG on the higher catalytic activity of prepared Pt catalysts have been preliminarily discussed.

1. Introduction

The proton exchange membrane fuel cells (PEMFCs) have been the subject of great interest due to their potential application in electric vehicles and portable power sources [1–10]. However, there is one challenge for PEMFCs to face, which is to reduce the loading of precious metals (such as platinum) contained within PEMFC catalyst layers without undue expense of the performance. The traditional approaches to prepare electrodes for PEMFCs include painting, spraying, and printing of the inks consisting of prepared carbon supported catalyst (e.g. Pt/C and PtRu/C) and solubilized polymer electrolyte (such as Nafion® ionomer) onto either a gas diffusion layer or an electrolyte membrane [11,12]. But the Pt utilization in such conventional Nafion®-bonded electrodes is not very high, because of agglomeration of the Pt/C (or PtRu/C) particles [13]. Accordingly, it is crucial for the platinum particles to be located in the three-phase reaction zones for their utilization in promoting the reaction. It is the three-phase interface of catalyst, carbon and electrolyte that allows effective gas and water diffusion and proton transport and electron transport to and from the catalyst sites [14,15]. The catalyst particles inside the agglomerates are not in good contact with electrolyte phase, consequently, the catalyst is not fully utilized. There are some physical deposition methods, pulsed laser deposition (PLD) for example, it can not localize all the Pt particles where the electrocatalytic reaction takes place, and it will result in the decrease of Pt utilization. As well as this method requires expensive vacuum equipments [16]. Electrodeposition operates more easily and costs lower than others, and it makes it possible to deposit Pt catalysts selectively at desirable locations in the electrode with both ionic and electronic accessibility [13,17–19]. Nevertheless, it is difficult to maintain a small particle size of Pt deposition on the surface by conventional electrodeposition methods. After the formation of the initial Pt particles, further platinum reduction onto them is generally favored. If the size of the Pt particles prepared by electrodeposition decreases, the level of Pt utilization could be further improved. Therefore, it is possible to say that the electrodeposition can be a desirable method to fabricate platinized PEMFC electrodes. There are some methods used to control the particle size of electrodeposited Pt crystals. Kim et al. [20] improved the performance of the PEMFC electrodes by controlling the pulse deposition parameters such as the peak current density, the pulse duty cycle and the total charge density. They pointed out that the peak current density and duty cycle could control the nucleation rate and decrease the catalyst dendritic growth. Their results show that when the Pt loading is 0.7 mg cm^{-2}, the specific active surface reaches 33 m^2 g^{-1}. Bennett et al. [21] reported pulsed galvanostatic deposition of nanometer-sized Pt particles on electrically conducting microcrystalline and nanocrys-

* Corresponding author. Tel.: +86 10 623 32651; fax: +86 10 623 32265.
E-mail address: echem@ustb.edu.cn (X. Wang).

0378-7753/$ – see front matter © 2008 Published by Elsevier B.V.
doi:10.1016/j.jpowsour.2008.07.025

talline diamond thin-film electrodes. The separate depletion layers on the diamond around each Pt particle result in similar growth rates and lead to more highly dispersed particles with smaller size. Pt catalyst deposited at 1 s pulses (duty cycle 50%) and current density 1.5 mA cm^{-2} displays a electrochemically active area of $0.18 \pm 0.04\ cm^{-2}$ (electrode area is $0.2\ cm^{-2}$). And the coverage of Pt particles needs to be further improved.

The Seeded-growth approach has been developed to produce nanoparticles, such as silver, ZnO and Cu [22–24]. In addition, it has been shown that the organic additives play important roles in preparing nanomaterials [25,26]. In recent years, polyethoxylated compounds are used widely in the electrodeposition of copper and zinc as nonionic surfactant additives, because of their selective adsorption property. PEG is added in electrolytic baths to influence crystal growth and modify the morphology of ZnO nanocrystallite [27]. A useful technique may be induced from these two tactics for the preparation of other nanoscale materials via electrodeposition methods.

In this study, a new pulse electrodeposition method for Pt nanoparticles is pointed out, which combines coating Pt seeds on the C-Nafion substrate and introducing polyethylene glycol (PEG) into the deposition solution. This research aims to optimize the performance of the PEMFC electrodes and reduce the platinum loading in the electrode for oxygen reduction by controlling the particle size and morphology of Pt nanocrystallite. Firstly, we studied the effect of Pt seeds and PEG on the performance of catalyst prepared, respectively. Then we investigated the performance of electrode, which is prepared by Pt seeds and PEG. Finally, the optimized electrode was compared with a conventional electrode made from commercial 40% Pt/C catalyst.

2. Experimental

2.1. Fabrication of Pt/C-Nafion/graphite electrodes by electrodeposition

The process of fabricating Pt/C-Nafion/graphite electrodes by electrodeposition consisted of two steps. The first step was to make the C-Nafion/graphite electrodes without the electrodeposited Pt catalyst. And the second was pulse deposition of Pt on the C-Nafion substrates.

In the first step, 50 mg carbon black (Vulcan XC-72) with 200 μL Nafion® solution (5 wt.%, 45 mg cm^{-3}, DuPont) and 10 mL ethanol were mixed thoroughly in a supersonic bath. Then, 100 μL prepared ink was pipetted on a graphite electrode (diameter 8 mm), which was polished to mirror-like state and cleaned in ethanol and deionized water in advance. Then the electrode was dried at 50 °C for 8 h in a vacuum oven to vaporize the ethanol. The resulting C-Nafion/graphite electrode is served as the substrate for the Pt catalyst and named as Sub.

25 mg Pt/C (40 wt.%) catalyst, as Pt seeds, synthesized by the method mentioned in the literature [28] was dispersed ultrasonically in a mixed solution of 100 mL ethanol and 300 μL Nafion® solution (5 wt.%). Then, 50 μL prepared ink was pipetted onto the surface of Sub to form C-Nafion/graphite electrode with Pt seeds (named as Sub-Seeds). The loading of the Pt seeds is 10 μg cm^{-2}.

In the second step, four electrodes were fabricated. Electrode Blank represents the electrode elctrodeposited without Pt seeds and PEG. Electrodes Seeds and PEG were prepared with Pt seeds and PEG, respectively. And the Electrode fabricated with Pt seeds and PEG is named as Seeds&PEG. Electrodes Blank and Seeds were electrodeposited in 0.5 M H_2SO_4 + 1.0 mM H_2PtCl_6 on substrates Sub and Sub-Seeds, respectively. Electrode PEG and Seeds&PEG were electrodeposited in 0.5 M H_2SO_4 + 1.0 mM H_2PtCl_6 adding with 10^{-4} mM PEG-400 on Sub and Sub-Seeds, respectively. The concentration of PEG, deposition current density, on- and off-time were selected after series of experiments. The detailed preparation conditions were summarized in Table 1. After electrodeposition all electrodes were rinsed thoroughly with de-ionized water and dried at 50 °C in a vacuum oven.

2.2. Preparation of comparison electrode

A Pt/C-Nafion/graphite electrode made from commercial 40% Pt/C catalyst (Johnson Matthey) was used for comparison. The comparison electrode was fabricated by repeating all procedures of Sub in section 2.1 in place of Vulcan XC-72 with the commercial Pt/C catalyst. In order to ensure all electrodes in this paper possess similar hydrophilic-hydrophobic properties and porosities, the weight ratio of the carbon powder to Nafion® in solid form always remained about 1000:9. The Pt loading was 300 μg cm^{-2}.

2.3. Electrochemical measurement

All the electrochemical experiments were performed using Potentiostat of Princeton Applied Research Model VMP2 at 30 °C. A conventional three-electrode cell was used in these experiments. Pt sheet and a saturated calomel electrode (SCE) were used as counter electrode and reference electrode, respectively. All potentials in this paper are quoted with reference to SCE.

Cyclic voltammetry (CV) in 0.5 M H_2SO_4 between −0.25 and 1.1 V with scan rate of 100 mV s^{-1} was used to determine the electrochemically active surface area of the Pt catalysts. Prior to CV experiments pure argon was passed through the electrolyte solution to remove oxygen dissolved in it. The CVs were tested till a reproducible curve was acquired.

Activity of the samples for ORR was studied with Model636 rotating disk electrode in O_2-saturated 0.5 M H_2SO_4. The potential was swept from 0.9 to 0.1 V at 5 mV s^{-1}.

2.4. Physical characterization

The prepared catalysts were characterized for particle morphology using Scanning electron microscopy (ZEISS and LEO-1530 FESEM). X-ray diffraction (XRD) measurement was measured by MXP21 VAHF system (Cu Kα/35 kV/200 mA).

Platinum loadings of the electrodes were determined by using a WFZ UV-2100PC spectrophotometer. The carbon layer on the surface of the electrode prepared was scratched into a quartz crucible. Carbon was removed from the sample by burning at 800 °C for 30 min. The residue was dissolved in 4 mL aqua regia ($3Pt + 4HNO_3$ +

Table 1
Preparation conditions for the Pt catalysts

Electrode	Substrate	Concentration of PEG (mM)	Total charge density (C cm^{-2})	Deposition current density (mA cm^{-2})	On-time (s)	Off-time (s)
Blank	Sub	0	1.2	−0.6	1	5
Seeds	Sub-Seeds	0	1.08	−0.6	1	5
PEG	Sub	10^{-4}	1.2	−0.6	1	5
Seeds&PEG	Sub-Seeds	10^{-4}	1.08	−0.6	1	5

$18HCl = 3H_2[PtCl_6] + 4NO + 8H_2O$). The solution obtained was evaporated almost to dryness. 5 mL HCl (6.8 M) was added and transferred into a volumetric flask. Then 1.25 mL $SnCl_2$ (1 M) was added and the solution was made up to the mark with 2 M HCl. The absorbance of the solution was measured at 402 nm against the blank. The concentration of platinum was calculated using the appropriate regression equation.

3. Results and discussion

3.1. Electrode deposited with Pt seeds

Fig. 1 shows the SEM images of Sub, Sub-Seeds, electrodes Blank and Seeds. In comparison with the micrograph of Sub, it can be seen that the diameter of Pt seeds is less than 5 nm. Electrode Blank shows spherical Pt clusters with different sizes ranging from 100 to 600 nm. This indicates that the Pt nuclei are formed in different stages during the deposition process on Sub. Electrode Seeds shows clump-like Pt crystal formations with average particle size 100 nm. The interfacial tension between solution species and a crystal nucleation site depends on the degree of structural fit, and the same crystal type has the best fit and the lowest energy barrier [29]. The SEM images of electrode Seeds reveal that pre-coating the substrate with Pt seeds, the same material as the nanocrystals being grown, yields Pt deposit with changed morphology. Furthermore, electrode Seeds has much better dispersion and coverage of Pt than electrode Blank. Pre-coating the substrate with Pt seeds can increase the number of Pt crystal nucleus. In that case, the rate of nucleus formation is probably higher than that of nucleus growth. As a result, more and smaller Pt nanocrystals are obtained. The Pt loading W determined by spectrophotometry on electrode Seeds is 186.6 $\mu g\,cm^{-2}$, higher than that of Blank (122.0 $\mu g\,cm^{-2}$). The deposition current efficiency of electrodes Blank and Seeds are 20.3% and 32.7%, respectively (see Table 2). Introduction of Pt seeds before deposition step is a key factor in determining the final Pt deposit.

Fig. 2 shows cyclic voltammograms of Sub-Seeds, Blank and Seeds in 0.5 M H_2SO_4. The shapes of the CVs for Blank and Seeds

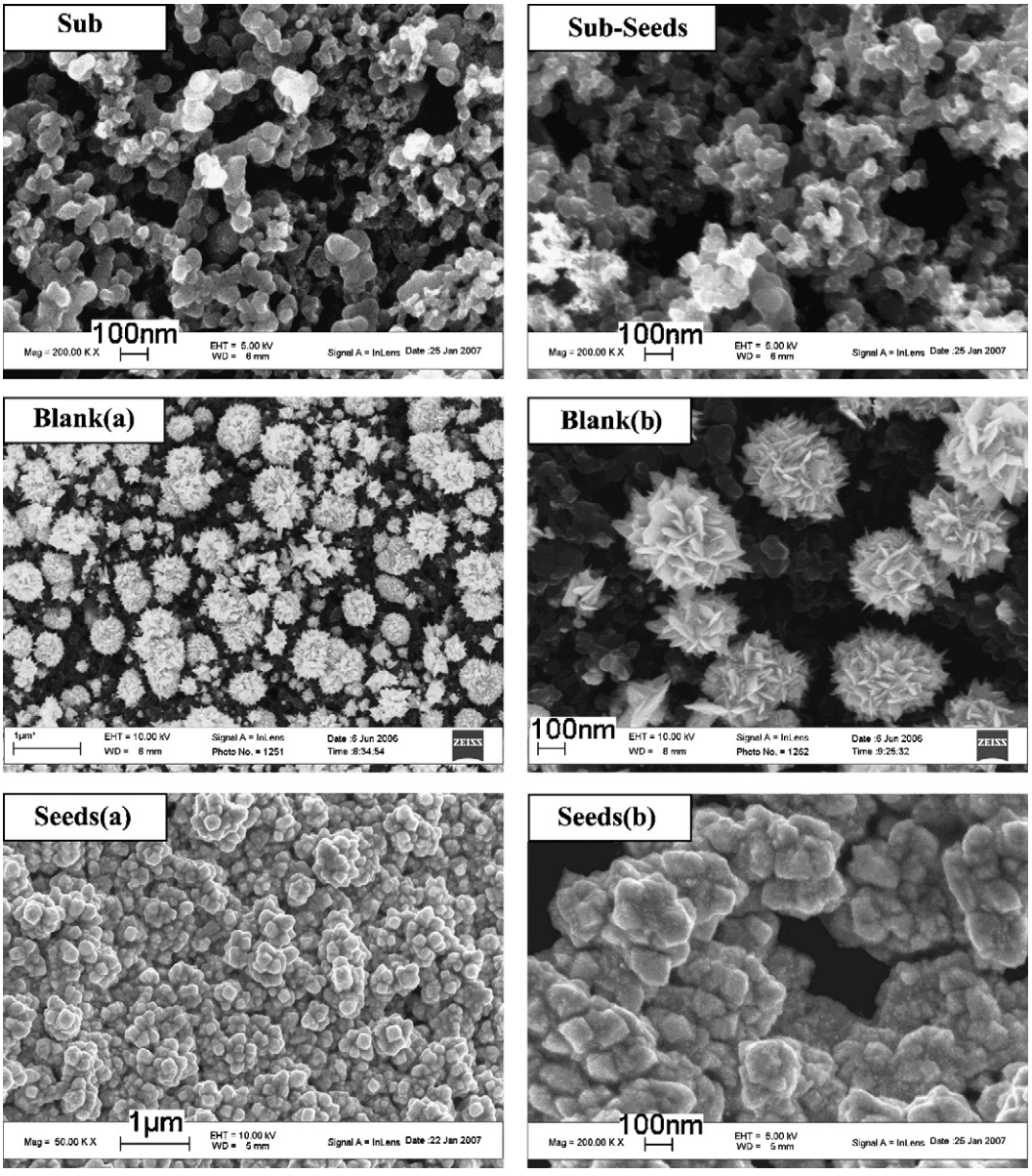

Fig. 1. Scanning electron micrographs of substrates Sub, Sub-Seeds and electrodes Blank and Seeds. Mag = 50.00 K×; (b) Mag = 200.00 K×.

Table 2
Platinum loading, surface area and peak currents for the prepared electrodes

Electrode	W^a ($\mu g\,cm^{-2}$)	η^b (%)	$A_s{}^c$ ($cm^2_{Pt}\,cm^{-2}_{graphite}$)	S^d ($m^2\,g^{-1}$)	d^e (nm)	$I_D{}^f$ ($mA\,cm^{-2}$)	$A_s/A_{s-Blank}{}^g$	$I_D/I_{D-Blank}{}^h$
Blank	122.0	20.3	28.0	22.9	10.2	3.04	1.00	1.00
Seeds	186.6	32.7	38.7	20.7	11.3	4.23	1.38	1.39
PEG	199.0	33.1	52.7	26.5	8.8	5.50	1.88	1.81
Seeds&PEG	225.0	39.5	78.7	35.0	6.7	7.35	2.81	2.42

[a] Pt loading determined by spectrophotometry.
[b] Current efficiency.
[c] Electrochemically active specific surface area of Pt per unit area of graphite electrode.
[d] Mass specific surface area: electrochemically active specific surface area per unit weight of Pt.
[e] Pt particle size calculated from Eq. (1).
[f] The diffusion limited current density of RDE cathodic curves.
[g] The ratio of the electrode's A_s to the A_s of electrode Blank.
[h] The ratio of the electrode's I_D to the I_D of electrode Blank.

are similar to that of polycrystalline Pt [30]. Two reversible hydrogen adsorption/desorption peaks are clearly distinguished in the potential region from 100 to −250 mV.

The measurement of the electrochemically active surface area of the Pt catalyst is critical for evaluating its catalytic activity. The electrochemical surface area of a Pt catalyst is usually determined from the adsorption/desorption charge of hydrogen atoms measured by cyclic voltammetry. The H adsorption charge density was evaluated by integrating the cathode current for hydrogen adsorption reaction and correcting for the double-layer charging current (see the shaded region of the *I–E* curve in Fig. 2) [31]. For a polycrystalline Pt electrode, the charge associated with the above reaction is 210 $\mu C\,cm^{-2}$ [32]. The electrochemically active areas of Pt for electrodes Blank and Seeds, which is normalized to the geometric area of the graphite electrode, are 27.96 and 38.71 $cm^2_{Pt}\,cm^{-2}_{graphite}$, respectively. A summary of the particle analysis data was presented in Table 2. Assuming a cubic structure of the Pt deposit with five faces exposed to the electrolyte, an average particle size d (nm), the loading W ($\mu g\,cm^{-2}$) and electrochemically active specific surface area A_s ($cm^2_{Pt}\,cm^{-2}_{graphite}$) have relationship as follows [33]:

$$d = 2.336 \times \frac{W}{A_s} \quad (1)$$

This equation was used to calculate the average particle size in Table 2.

The platinum particle sizes observed with the SEM are much larger than those calculated from the electrochemical measurements (Table 2). This probably because that the Pt clusters consist of smaller particles as observed by Ye and Fedkiw [33]. For Electrode Blank, the particle sizes observed range from 100 to 600 nm. But the particle size d calculated however is only 10.2 nm. This can be attributed to a fine structure roughness of Pt. Each spherical Pt cluster consists of many flakes, which results in a high value of electrochemically active specific surface area A_s. Therefore, a small value of d is obtained according to Eq. (1), so is electrode Seeds. The clumps are about 100 nm in diameter with small steps on them, which is larger than the value of d calculated (11.3 nm).

Fig. 3 shows RDE cathodic curves for substrates Sub, Sub-Seeds and electrodes Blank and Seeds&PEG in O_2-saturated 0.5 M H_2SO_4. For comparison, the voltammetric responses for substrates Sub and Sub-Seeds are also shown in Fig. 3. Few oxygen reduction current is observed on Sub within the study potential range. This means that the carbon substrate has no obvious electrocatalytic activity for ORR. Sub-Seeds displays low electrocatalytic activity (1.42 $mA\,cm^{-2}$) for ORR. The values of diffusion limited current density of RDE cathodic curves, I_D, are listed in Table 2. In order to facilitate comparison, all the values of I_D were recorded at the potential of 0.1 V. The value I_D of electrode Seeds is 4.23 $mA\,cm^{-2}$, which is lager than that of electrode Blank (3.04 $mA\,cm^{-2}$). According to Table 2, for electrode Seeds the value of $A_S/A_{S-Blank}$ is the same as that of $I_D/I_{D-Blank}$. As a result, such an improvement may be attributed to the higher electrochemically active Pt area of electrode Seeds.

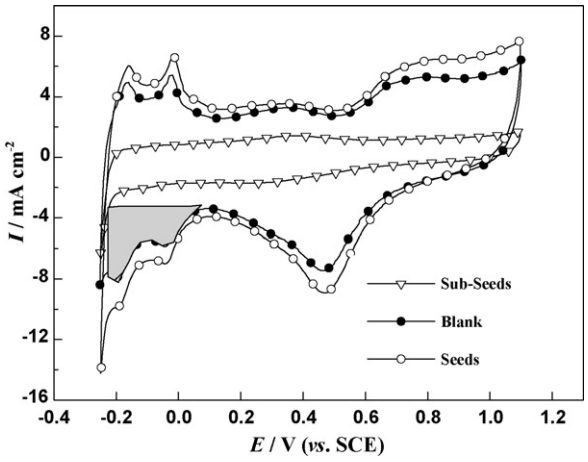

Fig. 2. Cyclic voltammograms (100 $mV\,s^{-1}$) of substrate Sub-Seeds and electrodes Blank and Seeds in 0.5 M H_2SO_4. The shaded region of the curve represents the charge associated with hydrogen adsorption.

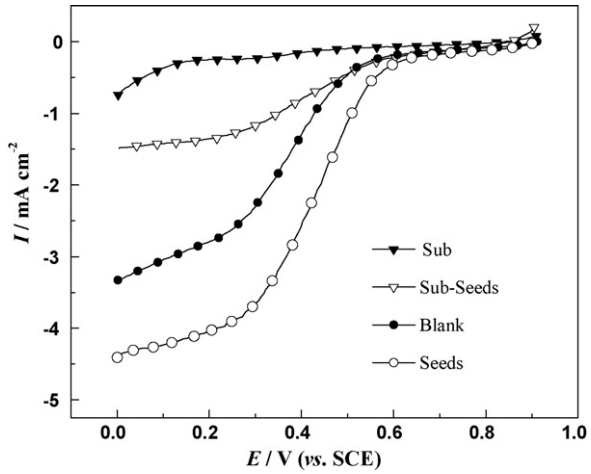

Fig. 3. RDE cathodic curves for substrates Sub, Sub-Seeds and electrodes Blank and Seeds in O_2-saturated 0.5 M H_2SO_4. Sweep rate 5 $mV\,s^{-1}$. Rotation speed 2500 rpm.

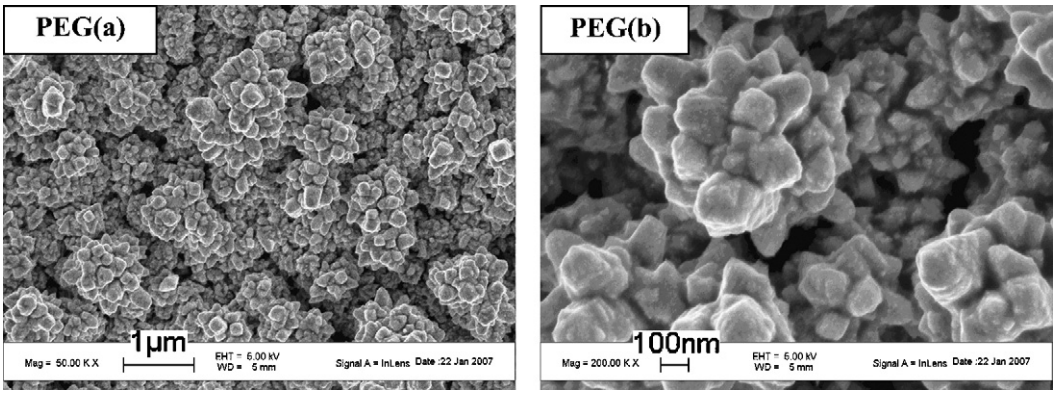

Fig. 4. Scanning electron micrographs of electrode PEG. (a) Mag = 50.00 K×; (b) Mag = 200.00 K×.

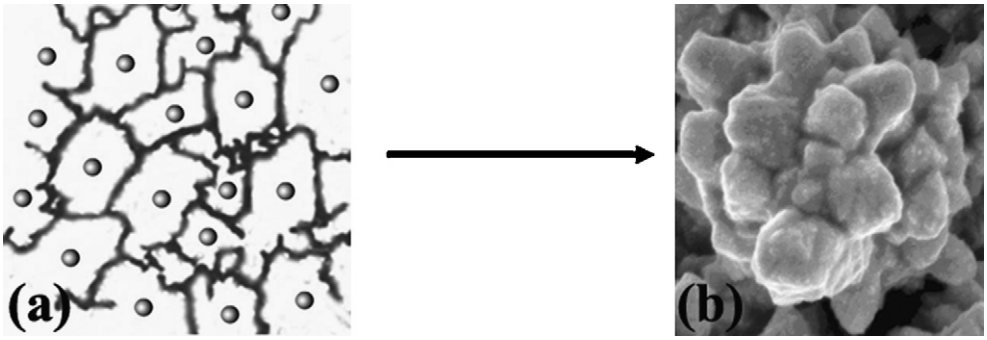

Fig. 5. Schematic representation of the growth of crystal nuclei surrounded by PEG polymer chain.

3.2. Electrode deposited with PEG

Fig. 4 shows the SEM images of electrode PEG. The particle size and morphology of Pt deposit are affected by the shape-controlled agents. From the micrograph of electrode PEG, we note that addition of PEG-400 yields clump-like crystal formations. The clumps range from 20 to 100 nm with many small steps on them.

In general, PEG is usually used as a surfactant due to its selective adsorption to inhibit crystal growth and modify the morphology of nanocrystallite. In water the chains may intertwist with others and then become a network structure [34], as seen in Fig. 5(a). PEG can provide a new sort of organization to metal atoms along the polymer backbone, which affords the novel assembling ways for the clumps growth of the final product. During the electrodeposition, Pt adatoms enter the active sites on the surface of porous C-Nafion electrode. Then these Pt nuclei are immediately and strongly absorbed and surrounded completely by PEG chain (Fig. 5(a)). The PEG polymer surrounding the crystal nuclei of platinum prevents their growth and generates the steric hindrance effect leading to reduced particle–particle aggregation [35]. And the facet with a higher density of surface atoms is blocked by the adsorption of surfactants during the crystal growth, and the growth along this facet is considerably restricted. Under this environment, the pulse electrodeposited platinum nucleation is limited to the epitaxial mircroenvironment and naturally prefer to grow along PEG chains, which results in the growth of platinum clump [36], as shown in Fig. 5(b). We think that PEG-400 molecule's soft template assembly is a pivotal factor, despite the detail is awaited for further investigation.

Fig. 6 shows cyclic voltammogram in 0.5 M H_2SO_4 for electrode PEG. The CV shows features characteristic to the polycrystalline Pt. The electrochemically active specific area of electrode PEG is 52.7 $cm^2_{Pt}\ cm^{-2}_{graphite}$, as seen in Table 2. The electrochemically active Pt area of electrode PEG is 1.88 times that of electrode Blank, as expected from its smaller particle size (8.8 nm) and higher electrodeposition efficiency of platinum (33.1%), as shown in Table 2.

Fig. 7 shows RDE cathodic curves for Sub and electrode PEG in O_2-saturated 0.5 M H_2SO_4. The diffusion limited current density of electrode PEG is 5.5 mA cm^{-2}, which is almost twice as much as that of electrode Blank.

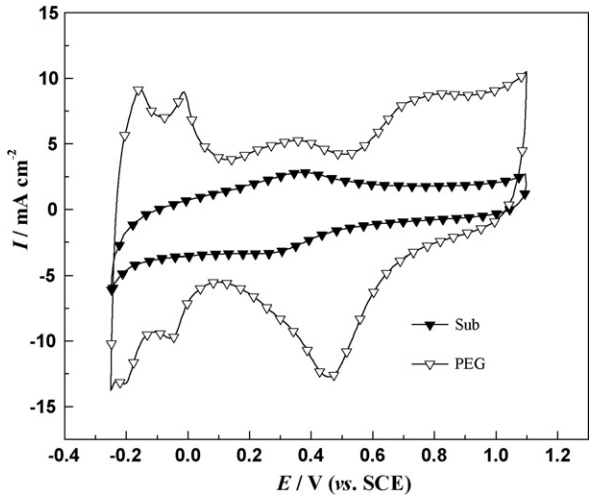

Fig. 6. Cyclic voltammograms (100 mV s^{-1}) of substrate Sub and electrode PEG in 0.5 M H_2SO_4.

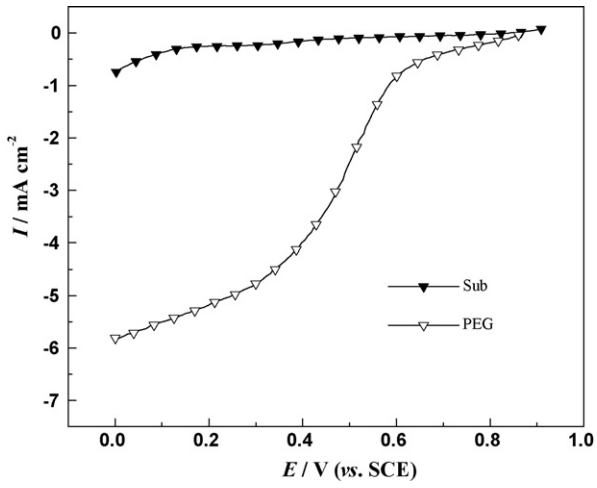

Fig. 7. RDE cathodic curves for substrate Sub and electrode PEG in O_2-saturated 0.5 M H_2SO_4. Sweep rate 5 mV s^{-1}. Rotation speed 2500 rpm.

Table 3
The intensity ratios of electrodes fabricated by pulse electrodeposition

Electrode	Blank	Seeds	PEG	Seeds&PEG
(1 1 1)/(2 2 0)	4.65	4.64	6.05	5.56
(2 0 0)/(2 2 0)	1.65	1.82	2.02	2.25

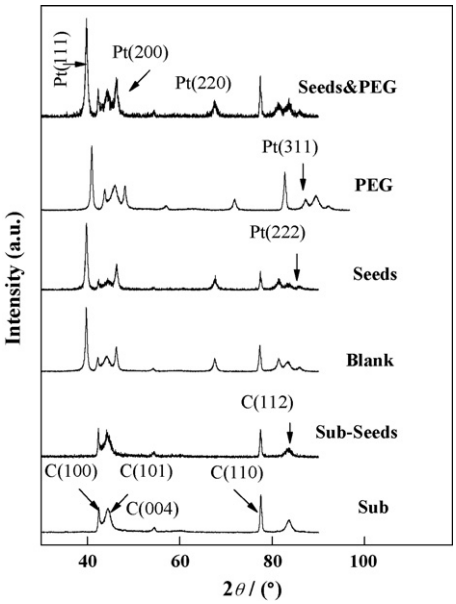

Fig. 9. X-ray diffraction patterns of the different substrates Sub, Sub-Seeds and electrodes Blank, Seeds, PEG and Seeds&PEG.

3.3. Electrode deposited with Pt seeds and PEG

Fig. 8 exhibits SEM images of electrode Seeds&PEG. Seeds&PEG displays elongated leaf-like flake clusters. These flakes are about 100–200 nm in length and have sharp tips.

Fig. 9 is the XRD patterns for the pulse electrodeposited electrodes. The reflectance peaks of the Sub and Sub-Seeds between 30°and 90° are indexed to a graphite phase (PDF number 1-640). The diffraction peaks of four electrodes at about 39°, 46°, 68°, 81°and 86°are due to Pt (1 1 1), (2 0 0), (2 2 0), (3 1 1) and (2 2 2) plane, respectively, which represents the typical character of a platinum fcc structure. In the (2 2 0) peak region there are no reflection signals associated with the carbon substrate, and the (1 1 1)/(2 2 0) and (2 0 0)/(2 2 0) intensity ratios are calculated and listed in Table 3. From Table 3, it can be seen that the intensity ratios of electrode Seeds are almost the same as those of electrode Blank, indicating that introduction of Pt seeds on the substrate has almost no effect on the growth direction of Pt crystallites that consist of the polycrystalline Pt, while PEG-400 has influence on it to some extent.

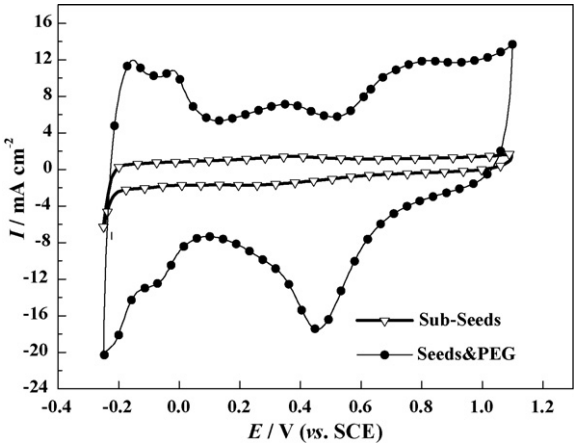

Fig. 10. Cyclic voltammograms (100 mV s^{-1}) of substrate Sub-Seeds and electrode Seeds&PEG in 0.5 M H_2SO_4.

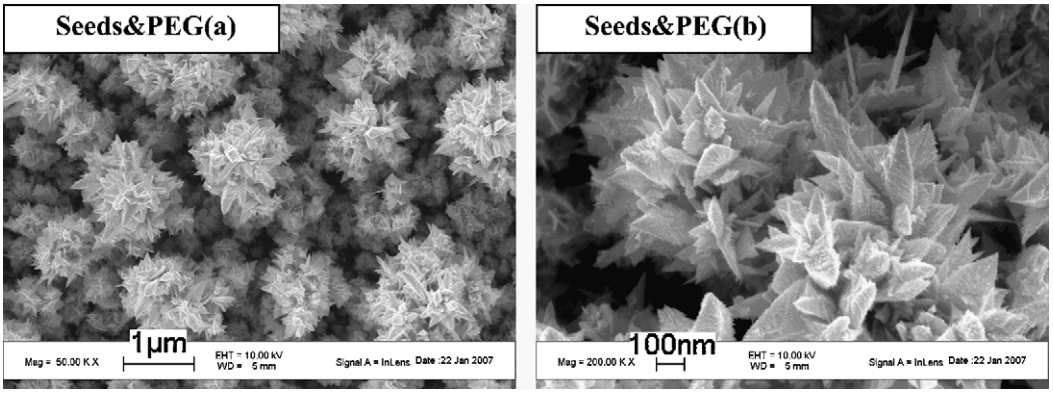

Fig. 8. Scanning electron micrographs of electrode Seeds&PEG. (a) Mag = 50.00 K×; (b) Mag = 200.00 K×.

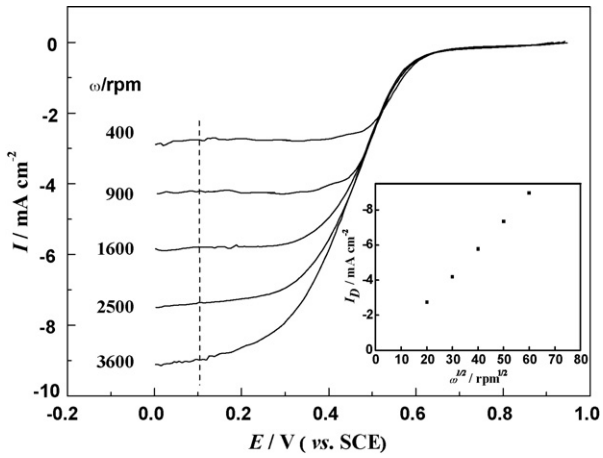

Fig. 11. RDE voltammetry results for O_2 reduction on electrode Seeds&PEG in O_2-saturated 0.5 M H_2SO_4. Sweep rate 5 mV s^{-1}. Inset: Levich plots for O_2 reduction on electrode Seeds&PEG in O_2-saturated 0.5 M H_2SO_4 at 0.1 V vs. SCE.

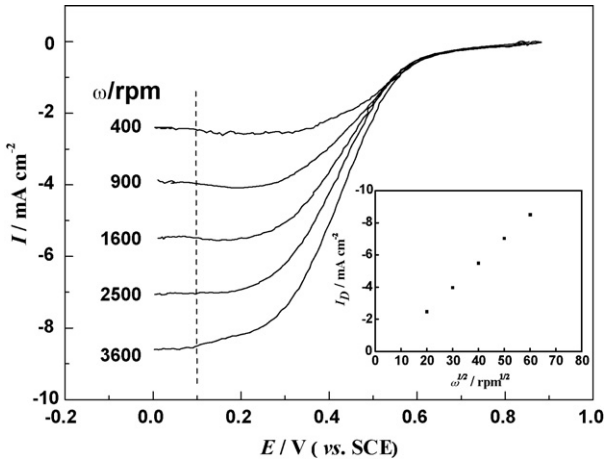

Fig. 12. RDE voltammetry results for O_2 reduction on electrode Pt/C–C in O_2-saturated 0.5 M H_2SO_4. Sweep rate 5 mV s^{-1}. Inset: Levich plots for O_2 reduction on electrode Pt/C–C in O_2-saturated 0.5 M H_2SO_4 at 0.1 V vs. SCE.

Fig. 10 shows cyclic voltammograms in 0.5 M H_2SO_4 for electrode Seeds&PEG. The voltammogram of the electrode is consistent with that of polycrystalline Pt. The electrochemically active specific surface area of Seeds&PEG is 78.7 $cm^2_{Pt}\ cm^{-2}_{graphite}$, as shown in Table 2. The Pt particle size calculated is 6.7 nm, much smaller than that observed from the micrograph. Among four electrodes studied, Seeds&PEG. has the largest mass specific surface area of 35.0 $m^2\ g^{-1}$ (electrochemically active specific surface area per unit weight of Pt).

The electrochemical reduction of oxygen on electrode Seeds&PEG was studied in O_2-saturated 0.5 M H_2SO_4 by using RDE. The representative current-potential curves of various rotation speeds are presented in Fig. 11. For Seeds&PEG the diffusion limited current density I_D at 2500 rpm is 7.35 mA cm^{-2}, which is almost three times as much as that of Blank. Conventional results from a rotating disk voltammetry experiment can be interpreted using the well-known Levich equation [37]; i.e.:

$$I_D = 0.620nFD^{2/3}\omega^{1/2}\nu^{-1/6}C \quad (2)$$

where I_D is the diffusion limited current density, ω is the rotation speed (rpm), ν is the kinematic viscosity, and all other symbols have their usual significance. The inset of Fig. 11 shows some Levich plots (I_D vs. $\omega^{1/2}$) determined from the current-potential curves, where the current recorded at the potential 0.1 V was used as the diffusion limiting current. From Eq. (2), the linear sloping plot of I_D vs. $\omega^{1/2}$ (that passes through the origin) indicates that the system being examined is under mass transport control.

From Table 2 we can see that electrode Seeds&PEG exhibits a better catalysis to ORR and the A_s/A_{s-A} and I_p/I_{p-A} values of the four electrodes are very close, indicating that the increase in the electrocatalytic activities may be attributed to higher active surface area of the Pt catalyst.

Electrode Seeds&PEG was chosen to be compared with a conventional electrode made from commercial Pt/C catalyst. The characteristics of ORR on comparison electrode are presented in Fig. 12. From the inset of Fig. 12, we can see that the commercial Pt/C–C is also under mass transport control. Loadings of Pt on electrodes Pt/C–C and Seeds&PEG are 300 and 225 $\mu g\ cm^{-2}$, respectively. The current at the same rotation speed on electrode Seeds&PEG is higher than that on electrode Pt/C-C. At rotation speed 400 rpm, the values of diffusion limited current density I_D on Seeds&PEG and Pt/C–C are 2.75 and 2.47 mA cm^{-2}, respectively. And at rotation speed 2500 rpm, the values of I_D on Seeds&PEG and Pt/C–C are 7.35 and 7.02 mA cm^{-2}, respectively. The performance of electrode Seeds&PEG with loading of 225 $\mu g\ cm^{-2}$ is better than the conventional electrode Pt/C–C with loading of 300 $\mu g\ cm^{-2}$.

4. Conclusions

The electrodeposition method is a simple, efficient way to produce platinum or metallic nanoparticles. PEMFC electrode with improved performance was fabricated by a new pulse electrodeposition method. Introducing PEG-400 in deposition solution and coating the C-Nafion substrate with Pt seeds can control the crystallite morphology and further decrease the particle size of Pt deposition. The average particle size of the Pt particles electrodeposited by introducing PEG-400 and Pt seeds is 6.7 nm and the mass specific surface area of Pt is 35.0 $m^2\ g^{-1}$. The performance of the electrode fabricated by using PEG-400 and Pt seeds with Pt loading of 225 $\mu g\ cm^{-2}$ is better than the conventional electrode with Pt loading of 300 $\mu g\ cm^{-2}$. The currently revealed technique should be very useful in the design and fabrication of PEMFC electrodes by means of electrodeposition method.

Acknowledgements

This project was funded by The National Nature Science Foundation of China (No. 50528404) and The Grant 863 Program of China (2006AA03Z224 and 2007AA05Z150).

References

[1] L. Liu, C. Pu, R. Viswanathan, Q. Fan, R. Liu, E.S. Smotkin, Electrochim. Acta 43 (1998) 3657–3663.
[2] B.D. McNicol, D.A.J. Rand, K.R. Williams, J. Power Sources 83 (1999) 15–31.
[3] K.B. Prater, J. Power Sources 61 (1996) 105–109.
[4] X.M. Ren, M.S. Wilson, S. Gottesfeld, J. Electrochem. Soc. 143 (1996) L12–L15.
[5] D.H. Jung, C.H. Lee, C.S. Kim, D.R. Shin, J. Power Sources 71 (1998) 169–173.
[6] F. Vigier, C. Coutanceau, A. Perrard, E.M. Belgsir, C. Lamy, J. Appl. Electrochem. 34 (2004) 439–446.
[7] M.P. Hogarth, T.R. Ralph, Platinum Met. Rev. 46 (2002) 146–164.
[8] D. Harvey, J.G. Pharoah, K. Karan, J. Power Sources 179 (2008) 209–219.
[9] Y. Zhang, H.M. Zhang, Y.F. Zhai, X.B. Zhu, C. Bi, J. Power Sources 168 (2007) 323–329.
[10] H.S. Chu, F.H. Tsau, Y.Y. Yan, K.L. Hsueh, F.L. Chen, J. Power Sources 176 (2008) 499–514.
[11] A.J. Dickinson, L.P.L. Carrette, J.A. Collins, K.A. Friedrich, U. Stiming, Electrochim. Acta 47 (2002) 3733–3739.
[12] S. Wasmus, A. Kuver, J. Electroanal. Chem. 461 (1999) 14–31.
[13] S.D. Thompson, L.R. Jordan, M. Forsyth, Electrochim. Acta 46 (2001) 1657–1663.
[14] Z.D. Wei, H.B. Ran, X.A. Liu, Y. Liu, C.X. Sun, S.H. Chan, P.K. Shen, Electrochim. Acta 51 (2006) 3091–3096.
[15] G. Lister, G. McLean, J. Power Sources 130 (2004) 61–76.

[16] L.H. Joo, G.M. Choi, J. Eur. Ceram. Soc. 27 (2007) 4273–4277.
[17] Z.D. Wei, S.H. Chan, L.L. Li, H.F. Cai, Z.T. Xia, C.X. Sun, Electrochim. Acta 50 (2005) 2279–2287.
[18] F. Montilla, E. Morallón, I. Duo, Ch. Comninellis, J.L. Vázquez, Electrochim. Acta 48 (2003) 3891–3897.
[19] H.S. Kim, B.N. Popov, Electrochem. Solid State Lett. 7 (2004) A71–A74.
[20] H.S. Kim, N.P. Subramanian, B.N. Popov, J. Power Sources 138 (2004) 14–24.
[21] J.A. Bennett, Y. Show, S. Wang, G.M. Swain, J. Electrochem. Soc. 152 (2005) E184–E192.
[22] S.J. Huo, X.K. Xue, Q.X. Li, S.F. Xu, W.B. Cai, J. Phys. Chem. B 110 (2006) 25721–25728.
[23] K. Yu, Z.G. Jin, X.X. Liu, J. Zhao, J.Y. Feng, Appl. Surf. Sci. 253 (2007) 4072–4078.
[24] H.F. Wang, Y.G. Yan, S.J. Huo, W.B. Cai, Q.J. Xu, M. Osawa, Electrochim. Acta 52 (2007) 5950–5957.
[25] S.J. Chen, X.T. Chen, Z.L. Xue, L.H. Li, X.Z. You, J. Cryst. Growth 246 (2002) 169–175.
[26] X. Ma, Z. Zhang, X. Li, Y. Du, F. Xu, Y. Qian, J. Solid State Chem. 177 (2004) 3824–3829.
[27] X.F. Zhou, D.Y. Zhang, Y. Zhu, Y.Q. Shen, X.F. Guo, W.P. Ding, Y. Chen, J. Phys. Chem. B 110 (2006) 25734–25739.
[28] L. Chen, M. Guo, H.F. Zhang, X.D. Wang, Electrochim. Acta 52 (2006) 1191–1198.
[29] R.B. Peterson, C.L. Fields, B.A. Gregg, Langmuir 20 (2004) 5114–5118.
[30] J.S. Gullón, E. Lafuente, A. Aldaz, M.T. Martínez, J.M. Feliu, Electrochim. Acta 52 (2007) 5582–5590.
[31] H. Qiao, M. Kunimatsu, T. Okada, J. Power Sources 139 (2005) 30–34.
[32] J. Wang, G.M. Swain, J. Electrochem. Soc. 150 (2003) E24–E32.
[33] J.H. Ye, P.S. Fedkiw, Electrochim. Acta 41 (1996) 221–231.
[34] W. Guo, G.S. Luo, Y.L. Wang, J. Colloid Interf. Sci. 271 (2004) 400–406.
[35] X.G. Wang, M.L. Wang, H. Song, B.J. Ding, Mater. Lett. 60 (2006) 2261–2265.
[36] F. Ye, L. Chen, J.J. Li, J.L. Li, X.D. Wang, Electrochem. Commun. 10 (2008) 476–479.
[37] C.J. Clarke, G.J. Browning, S.W. Donne, Electrochim. Acta 51 (2006) 5773–5784.